J Mol Model (2013) 19:2583–2591
DOI 10.1007/s00894-013-1792-1

ORIGINAL PAPER

Theoretical study of the thermodynamic and burning properties of oxygen-rich hydrazine derivatives—green and powerful oxidants for energetic materials

Peng Cheng Wang · Zhou Shuo Zhu · Jian Xu · Xue Jin Zhao · Ming Lu

Received: 12 November 2012 / Accepted: 5 February 2013 / Published online: 12 March 2013

Abstract A series of no-chlorine and oxygen-rich hydrazine derivatives (hydrazine modified with $–NO_2$ and NO_3^- groups) was designed and optimized to obtain molecular geometries and electronic structures at density functional theory–B3PW91/6−311++G(3df,3pd) level. Some important properties such as bond dissociation enthalpy, density, natural bond orbitals, thermodynamic parameters, molecular orbital energy and burning rate were then calculated. The simulation results revealed that these compounds exhibit excellent performance, with significant superiority over traditional oxidants found in propellants.

Keywords Oxidant · Hydrazine derivate · Density functional theory · Natural bond orbital · Burning rate

Introduction

Nowadays, there is great interest in developing new propellants for altitude rockets to allow heavier loading and farther launching distance [1–3]. However, despite the generation of several novel energetic materials (HMX, RDX, CL-20 and energetic salts) in the last century [4–7], for the most part, oxidants in propellants still employ ammonium nitrate (NH_4NO_3, AN) or ammonium perchlorate (NH_4ClO_4, AP) for many purposes. The disadvantages of these oxidants are obvious: the ability to supply oxygen and the combustion energy of AN is poor, thus weakening the efficiency of the propellant; and Cl in AP gives a high characteristic signal in military detection and would also cause severe atmospheric pollution [8–10]. Several improvements to AP have been witnessed, with products such as hydrazine perchlorate ($N_2H_5ClO_4$, HP), hydroxylamine perchlorate (NH_4OClO_4, HAP) and hydrazine diperchlorate [$N_2H_6(ClO_4)_2$, HP_2] being proposed. Although the combustion energy of oxidants was improved with these products, the other disadvantages noted above remain unsolved. Meanwhile, ever more frequent launching of rockets to outer space has meant a rapid growth in the Cl content in the atmosphere, leading to a potential safety hazard.

Anhydrous hydrazine has been considered an important resource in propellants due to its significant high energy per mole [11, 12]. But its other properties—it is toxic, inflammable and expensive—have limited its use to applications where there were no other choices. Researchers have taken two directions to attempt to improve this: (1) the synthesis of methyl derivatives such as monomethylhydrazine (MMH), 1,1-dimethylhydrazine (UDMH), 1,2-dimethylhydrazine (SDMH) and N-methyl-N-phenyl-hydrazine, which expand their application as energetic materials [13–18]; (2) the introduction of ClO_4^- or NO_3^- groups into molecular structures to develop them as oxidants. As yet, there are still only a few studies in this direction, with only one or two important compounds reported [19–24].

Here, we designed a series of oxygen-rich hydrazine derivatives by modifying hydrazine with $–NO_2$ and NO_3^- groups. As there was no carbon atoms and fewer hydrogen atoms, the ability to supply oxygen (measured by oxygen balance, OB_{100}) was excellent, reaching 39.2 OB_{100}. Also, the powerful energy export of hydrazine was developed and strengthened by the $–NO_2$ group. Since there was no Cl atoms, H_2O and N_2 (N_2O, NO and NO_2 reacted with

Electronic supplementary material The online version of this article (doi:10.1007/s00894-013-1792-1) contains supplementary material, which is available to authorized users.

P. C. Wang · Z. S. Zhu · J. Xu · X. J. Zhao · M. Lu (✉)
School of Chemical Engineering, Nanjing University of Science and Technology, Xiaolingwei 200,
Nanjing, Jiangsu Province 210094, China
e-mail: luming@mail.njust.edu.cn

Table 1 N–N bond dissociation enthalpies (BDEs) in hydrazine at different levels

	$E(NH_2NH_2)$ (a.u.)	$E(NH_2)$ (a.u.)	BDE (kJ mol^{-1})	ΔE (kJ mol^{-1})[c]
B3LYP/6−311 G++(3df,3dp)	−111.857740	−55.879890	257	19
B3LYP/aug-cc-pvdz	−111.830071	−55.865707	259	17
B3LYP/aug-cc-pvtz	−111.860300	−55.881374	256	20
CCSD/6-311++g	−111.356851	−55.637289	216	60
CCSD/6-311 G++(3df,3dp)	−111.682119	−55.789806	269	7
PW1PW91/6-311++G(3df,3pd)	−111.822683	−55.861214	263	13
B3PW91/6-311++G(3df,3pd)	−111.813353	−55.855836	267	9
G2MP2[a]			280	−4
Experimental[b]			276±8	

[a][53]
[b][54]
[c]Error between calculated and experimental value

energetic materials and formed N_2) would be the main products. So these hydrazine derivatives could be regarded as environmentally benign oxidants for the further development of novel propellants.

Methods

Computations were performed with the Gaussian 03 package using the B3PW91 [25–31] method with 6-311 G++ (3df,3pd) basis set [32]. The geometric parameters were allowed to optimize and no constraints were imposed on the molecular structure during the optimization process. Vibration frequencies were calculated for the optimized structures to enable us to characterize the nature of stationary points, zero-point energy (ZPE) and thermal correction. The volume was also calculated based on the optimized structures and iop(6/46) was set as 2,000 to minimize fluctuation. All optimized structures were characterized to be true local energy minima on potential energy surfaces without imaginary frequencies.

To measure bond strength and the relative stability of these molecules, the bond dissociation enthalpies (BDEs) of N–N bonds in each designed structure were calculated. BDE is the energy required for homolysis of a bond and is commonly denoted by the difference between total enthalpy of product and reactant after ZPE correction [33]. The expressions for the homolysis of bond A–B (1) and its BDE calculation (2) were shown as follows [34, 35]:

$$A - B(g) \rightarrow A \cdot (g) + \cdot B \cdot (g) \quad (1)$$

$$BDE(A - B)_H = E(A\cdot)_H + E(B\cdot)_H - E(A - B)_H \quad (2)$$

A–B stands for neutral molecules and A· and B· for the corresponding product radicals generated from bond dissociation; BDE (A–B) is the BDE of bond A–B; $E(A–B)_H$, $E(A\cdot)_H$, and $E(B\cdot)_H$ are ZPE-corrected total enthalpy of the parent compound and corresponding radicals, respectively.

An efficient and convenient statistics average method was worked out to predict the crystalline densities of energetic materials containing the elements C, H, N, and O [36–40]. To calculate the densities of nitramine compounds, the data of molecular volume was required. The molecular volume V was defined as inside a contour of 0.001 electrons/bohr3 density, which was evaluated using Monte–Carlo integration, where iop(6/46) was set to 2,000 to minimize fluctuation. The software Multiwfn [41] was used to contrast the reliability of volumes in Gaussian. The theoretical molecular density ρ (ρ=M/V, where M = molecular weight) was also calculated.

Table 2 $BDE_{(N–N)}$ and bond lengths of hydrazine derivatives

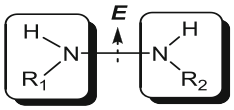

Compound	R_1	R_2	Bond length/Å	ΔE/kJ mol^{-1}
1	-H	-H	1.48	267
2	-H	$-NO_2$	1.37	367
3	-H	$-H\cdot HNO_3$	1.44	332
4	$-NO_2$	$-NO_2$	1.35	385
5	$-H\cdot HNO_3$	$-H\cdot HNO_3$	1.46	340
6	$-NO_2$	$-H\cdot HNO_3$	1.40	319[a]

[a]Value calculated at G2MP2 level

The OB_{100} was used to predict the oxygen delivery capacity of all oxidants, which represented the excessive O atom that the oxidant could supply. The supplied O atom helps explosive compounds to produce the most stable products (N_2, H_2O, CO, and CO_2) and thus release the highest energy. OB_{100} was calculated as follows:

$$OB_{100} = \frac{(O_{Total} - O_{Use})}{M} \times 1600 \quad (3)$$

where O_{Total} is the number of O atoms in the oxidant molecule, and O_{Use} the number of O atoms required in the oxidant itself during the reaction.

N—the number of moles of oxygen that oxidants could supply in unit volume—was calculated as follows:

$$N = \frac{\rho}{M} \times \frac{O_{Total} - O_{Use}}{2} \quad (4)$$

where ρ is the theoretical molecular density, and M the molecular weight; O_{Total} and O_{Use} were the same as in Eq. (3).

The burning rate μ(p), relative to the pressure and other factors when inflamed, was complex in real conditions, and was calculated as follows:

$$\mu(p) = K^* p\theta_0^2 \prod_{i=1}^{n} f_i h_l / \rho \quad (5)$$

K* was the constant in most conditions; f_i was the effect of every compound to the burning surface; h_l was the effect of every compound to the internal burning fire.

Here, we simplified its form to Eq. (6) [42, 43]. This equation does not show some details of burning but was exactly in accordance with its changing tendency.

$$\mu(p) = 1.709 p\theta_0^2 / \rho \quad (6)$$

ρ is the theoretical density of oxidant (g/cm^{-3}), and p is the pressure under current conditions (MPa). θ_0 is the mole fraction of molecular gas gaining oxidizing properties during burning and was calculated as follows:

$$\theta_0 = \frac{1}{\alpha + \beta + \gamma + q \times \eta(p) + 1} \quad (7)$$

α, β, γ and q differ for each oxidant. The detailed data and methods of evaluation can be found in the Supporting information. η(p) was calculated as follows:

$$\eta(p) = 2 - \exp 0.6931\left(1 - \frac{p}{p^*}\right) \quad (8)$$

p is the pressure under current conditions (MPa), and p* is characteristic pressure. This pressure was measured under conditions in which the compounds burned in an ideal state and were transformed completely into all the desired products. Different elemental composition in the propellant resulted in different p*. For propellants containing only N, H and O elements, the value of p was usually set at 9.81 MPa.

Results and discussion

N–N BDE and infrared spectra

The BDE of N–N not only affected the stability of hydrazine derivatives but also was the main source of explosive energy. Because there was no experimental data about the BDE of the designed compounds, we first used hydrazine as a typical substrate to scan the precision of different methods and basis sets. The value of BDE(N–N) in hydrazine is listed in Table 1. As can be seen, ab initio method G2MP2 was the closest to the experiment result, with a value of 280 kJ mol^{-1} of BDE(N–N), which could be regarded as the "gold standard" in bond energy calculation. Another method, CCSD, was closely related to the basis set and the addition of a diffuse function significantly improved precision. However, in that case, the cost in terms of time and computational resources would be no less than with G2MP2. With DFT methods, the error of B3LYP was still

Table 3 Some natural bond orbitals (NBOs) of hydrazine derivatives. Some of the data referred to is listed in this table; *LP* lone pair electrons; *BD* bonding orbital; *BD** antibonding orbital; *1*, *2*, *3* first, second and third lone pair electrons in each atom or bond between two atoms, respectively

Compound	Donor NBO (i)	Acceptor NBO (j)	Ei-j (kcal mol^{-1})
2			
N - NNO_2:	LP (1) N 1	BD*(1) N 2 - N 3	14.40
3			
N - OH:	LP (1) N	BD*(1) H - O	42.83
4			
N - NNO_2:	LP (1) N 2	BD*(1) N 3 - N 4	19.27
	LP (1) N 3	BD*(1) N 2 - N 1	19.23
5			
N - OH(5a):	LP (1) N 1	BD*(1) H - O	70.77
	LP (1) N 2	BD*(1) H - O	72.33
O - NH(5b):	LP (2) O	BD*(1) H - N 1	3.86
	LP (2) O	BD*(1) H - N 2	3.89
6			
N - NNO_2(6a):	LP (1) N 3	BD*(1) N 2 - N 1	12.99
N – OH(6a):	LP (1) N 3	BD*(1) H - O	45.30
O - NH(6b):	LP (1) O	BD*(1) H - N 2	3.43
	LP (2) O	BD*(1) H - N 2	3.32

very obvious even when we used the largest basis set, which meant it was not suitable here. PW91 performed better than B3LYP in this system. Especially B3PW91, whose BDE value was 267 kJ mol^{-1} with 9 kJ mol^{-1} error, was second only to "gold standard" G2MP2 and CCSD/6−311 G++ (3df, 3dp). Considering its lower cost compared to the ab initio method, and its acceptable precision, we chose B3PW91/6−311++G (3df, 3pd) as the basis set for further theoretical studies.

All designed hydrazine derivatives and their radicals formed in bond dissociation process were optimized at B3PW91/6−311++G (3df, 3pd) level. The $BDE_{(N-N)}$ and bond lengths were calculated and listed in Table 2. As can be seen, the introduction of the $–NO_2$ group could strongly improve the $BDE_{(N-N)}$ of **2** to 367 kJ mol^{-1} (37.5 % rise) and shorten the bond length to 1.37 Å, while the effect of the HNO_3 group in the form of salt was a little weaker than that of the $–NO_2$ group, with $BDE_{(N–N)}$ of **3** being 332 kJ mol^{-1} (24.3 % increase) and the bond length 1.44 Å. Yet, the change would be a little different when a second group was introduced. A second $–NO_2$ group would still strengthen its impact on the N–N bond. The

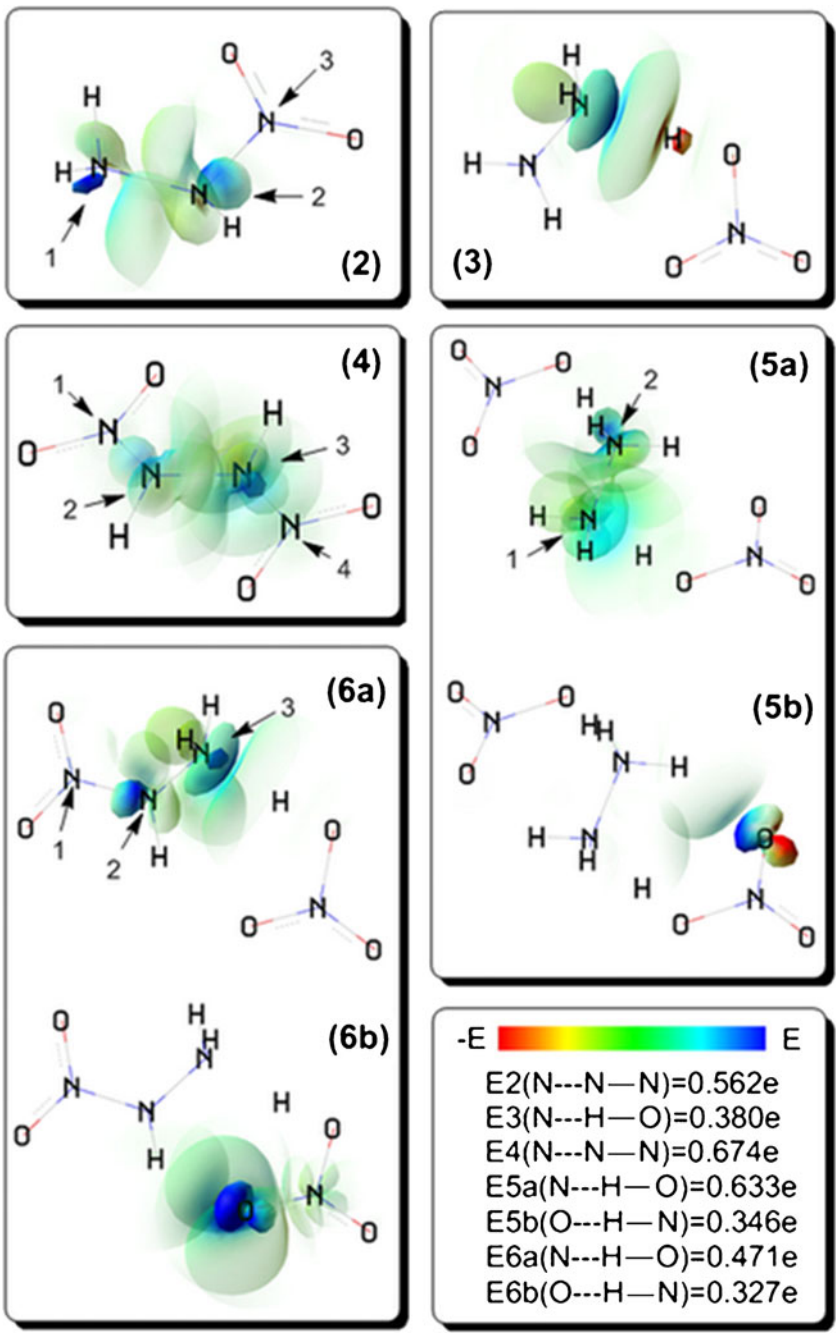

Fig. 1 Second order perturbation (SOP) of hydrazine derivatives

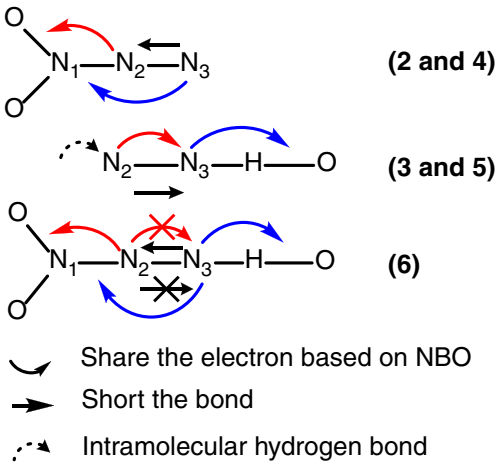

Scheme 1 Probable electron sharing conditions and bond length changes

$BDE_{(N-N)}$ of **4** reached the highest value of 385 kJ mol^{-1} and bond length was only 1.35 Å. Unexpectedly, a second HNO_3 group weakened the effect of the first, and the $BDE_{(N-N)}$ of **5** fell to 340 kJ mol^{-1} and the bond length was 1.46 Å. The $BDE_{(N-N)}$ of **6**, with two different groups, was only 7 kJ mol^{-1}, which is less than that of a hydrogen bond. We then calculated this $BDE_{(N-N)}$ at G2MP2 level; its value is 319 kJ mol^{-1} with the same structure.

To investigate the detailed interaction between introduced groups and hydrazine, natural bond orbital (NBO) was calculated with Gaussian 03. Some important results of intermediate compounds are listed in Table 3. Donor NBO (i) was the orbital that supplies electrons and acceptor NBO (j) was the orbital that accepts these electrons. Their interaction is described by the stabilization energy E_{i-j} based on second order perturbation (SOP) theory [44]. The higher the value of E_{i-j}, the stronger the interaction would be and thus the electrons were more likely to be shared by two orbitals. Furthermore, Fig. 1 presents a clear visual representation of this interaction based on the values in Table 3. E shows the intensity of interaction and its variation tendency was similar with E_{i-j}.

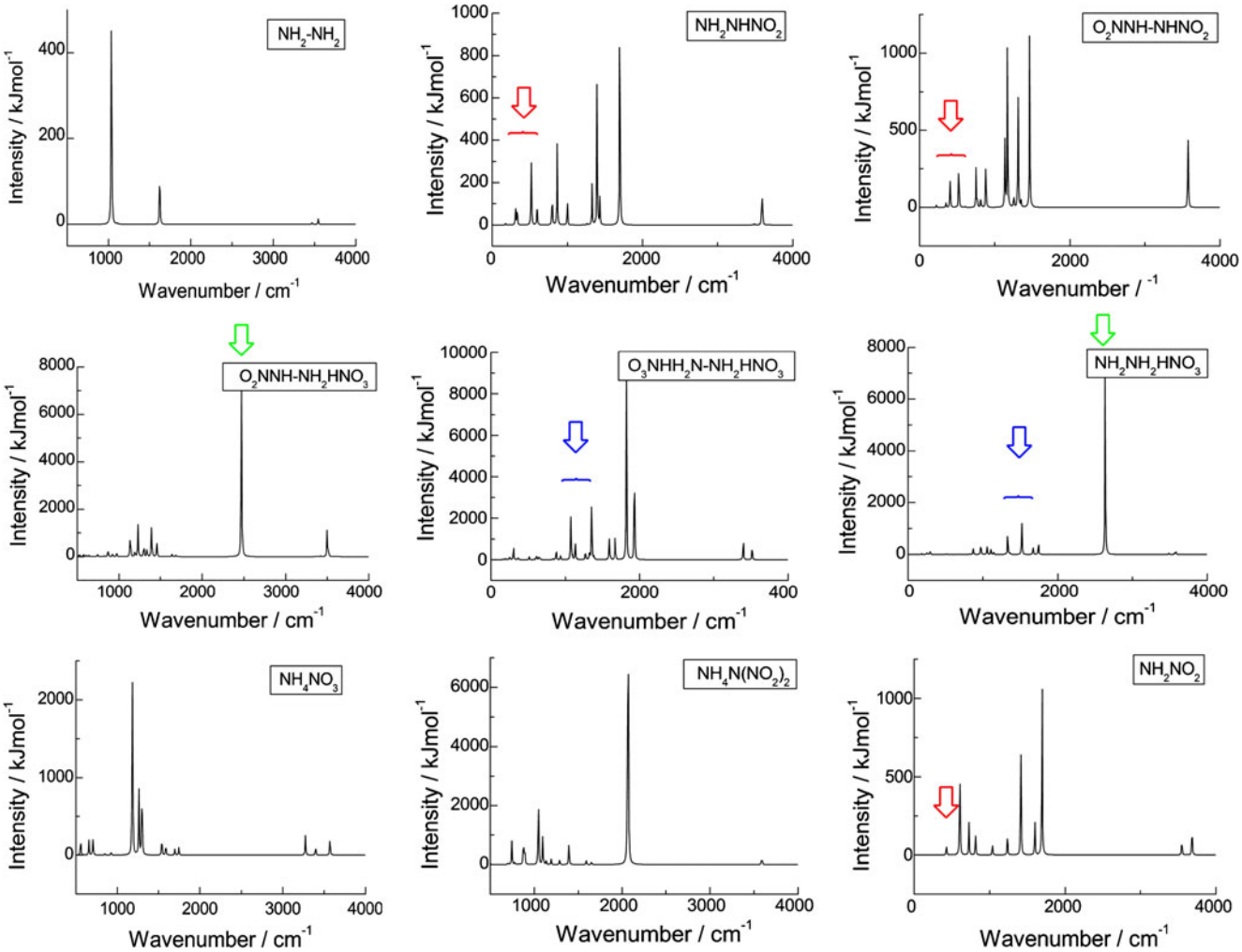

Fig. 2 Calculated infrared spectra of hydrazine derivatives

Table 4 Predicted densities, oxygen balance (OB) and gas volumes of hydrazine derivatives

Compound	V_a (cm^3 mol^{-1})	V_b (cm^3 mol^{-1})	ρ (g cm^{-3}) [a]	ρ′ (g cm^{-3})	OB_{100}	N (10^{-2}mol cm^{-3})
1	31.057	30.089	1.03	1.00[b]	−100	0
2	49.453	49.030	1.56	1.76[c]	10.4	1.00
3	63.833	63.725	1.49	1.69[b]	8.4	0.89
4	69.352	68.529	1.76	1.96[c]	39.2	2.41
5	97.420	96.947	1.62	1.82[c]	30.4	1.73
6	81.536	84.282	1.72	1.92[c]	34.3	2.06
7(AN)	53.804	54.107	1.49	1.72[b]	20	1.08
8(ADN)	78.003	78.298	1.59	1.81[b]	25.8	1.46
9(Nitramide)	39.809	37.007	1.56	1.78[b]	25.8	1.44

[a]Data calculated with Gaussian
[b]Experimental data
[c]Estimated data

As we know, the –NO_2 group is an electron-withdrawing group that would attract electrons from the atom it substituted. Yet, the –NO_2 group in **2** was obviously not satisfied with this situation as can be seen in Scheme 1; it tried to gain electrons from the N3 atom far from it because of the condition of electron deficiency over the whole molecule. This direct interaction between N1 and N3 was helpful in shortening the N–N bond and improving the bond energy. This effect was strengthened in **4** and thus the value of bond length was decreased to 1.35 Å with a highest $BDE_{(N–N)}$. In **3** and **5**, the HNO_3 group was not as strong as the –NO_2 group and shared the electron mainly with the N atom next to it. So, another N atom in hydrazine that was not affected would supply its electron to keep a balance, and an intramolecular hydrogen bond at this position was also helpful. This kind of bond shortening (as seen in Scheme 1) was different from the case with the –NO_2 group. The situation became complicated in **6** and we had to deduce its mechanism from the NBO results. Although there was still some effect of the –NO_2 group at N2 and N3, the HNO_3 group here also wanted to share the electron at N3, which weakened the connection between N1 and N3. Both these groups make N3 fall into a very electron deficient state. But here, N2, which was no better than N3, could not give any help as in **3** and **5**, since its electron was shared with N1-O. Thus, NBO judged the N2–N3 bond to be less energetic and only 319 kJ mol^{-1} was required to dissociate this bond.

Vibrational spectroscopy is one of the most important experimental tools in the study of unknown compounds, so information on calculated harmonic vibrational frequencies could be useful. Figure 2 shows the calculated IR spectra of different hydrazine derivatives obtained at B3LYP/6−311++G (3df, 3pd) level. Due to the complexity of vibrational modes, it was difficult to assign all bands. Therefore, only some typical vibrational modes were analyzed and discussed. The stretching and bending vibrational frequency of NH_4^+ and NO_3^- in AN was 3144 cm^{-1}, 1433 cm^{-1} and 1350 cm^{-1}, respectively; N–NO_2 peaks in ADN were at 1539 cm^{-1}, 1210 cm^{-1} and 1034 cm^{-1}. All these peaks could be found in the calculated infrared spectra. In **2** and **4**, the frequencies of the N-NO_2 group moved to short waves in some cases <500 cm^{-1} (red arrow). In **3** and **5**, the peak of NO_3^- moved to waves higher than 1500 cm^{-1} (blue arrow). When both -NO_2 and NO_3^- groups existed, as in **6**, the strong effect of -NO_2 inhibited the effect of NO_3^- and again moved the frequency to short waves (green arrow).

Densities, oxygen balance and gas formed

In this study, single-point molecular volume calculations at B3PW91/6−311++G (3df, 3pd) level were performed based on geometry optimized structures. Another software, Multiwfn, was also used here to check the results in Gaussian. As can be seen in Table 3, both tools showed a similar volume, and the error could be attributed mainly to the randomness of Monte-Carlo integration. Based on the volume, the density of hydrazine evaluated was 1.03 g/cm^3, which was very close to the experimental result of

Table 5 Calculated electronic energies (E_0), zero-point energies (ZPE) and enthalpies of formation (ΔH_f) in gas phase at G2MP2 level

Compound	E_0 (a.u.)	ZPE (a.u.)	H (a.u.)	ΔH_f (kJ/mol)
1	−111.673675	0.051429	−111.669071	97.06 (95)[a]
2	−315.936844	0.055978	−315.931084	91.69
3	−392.248888	0.081201	−392.240316	−110.23
4	−520.187087	0.059257	−520.179345	110.34
5	−672.818678	0.110359	−672.805438	−313.53
6	−596.502874	0.084847	−596.492265	−101.26
7	−337.025385	0.062802	−337.017534	−348.81
8	−521.395265	0.077114	−521.384604	−150.034
9	−260.699495	0.038989	−260.694880	−9.29
H_2O	−76.409524	0.021277	−76.326232	
NH_3	−56.527679	0.034289	−56.526735	

[a] Data from [54] in parenthesis

1.00 g/cm^3, whereas in dealing with the molecules that would form intermolecular hydrogen bonds, the densities would be underestimated. Some of these compounds have been successfully synthesized by now and their densities measured (see Table 3). Comparing the calculated and experimental results of **3**, **7**, **8** and **9**, we can see that their value difference was consistently about 0.2 g/cm^3. So we speculated that all the hydrazine derivatives would follow this rule, and predicted the densities of other compounds. Further experiments were designed to verify this presumed result.

OB was another of the most important criteria for selecting potential high energy and density oxidants. From Table 4, it can be seen that **4** has the highest OB among the hydrazine derivatives, with a value of 39.2 OB_{100}, 100 % higher than the traditional oxidant AN. Comparing **2** and **3**, **4** and **5**, it can be concluded that more substituents in the compound led to higher OB, and the oxygen supplying ability of compound containing a -NO_2 group was better than that containing a HNO_3 group. When the limit of admission space was considered, we used another index, N, to describe their properties: N = the number of moles of oxygen that oxidants could supply in unit volume. As can be seen, **4** continued its excellent performance because of its high density, with a value 130 % larger than that of AN. Those hydrazine derivatives with two substituents were also ahead of the others.

The computed electronic energies and enthalpies were also used to estimate the standard enthalpies of formation ($\Delta H°_f$) of hydrazine derivatives. There are two main pathways to calculate $\Delta H°_f$: the first is to design an isodesmic reaction [45–47]; the second uses atomization enthalpy [48–50]. Because the molecules are small enough, we can use atomization enthalpy and calculate their accurate enthalpies directly with the high level ab initio method G2MP2. By comparing the calculated and experimental result of **1** in Table 5, this method yielded acceptable results. As can be seen, $\Delta H°_f$ of most hydrazine derivatives was higher than traditional oxidants, which meant the oxidant itself could export more energy, and thus less energy would be required to active the reaction.

Thermal stability and burning rate

Stability here refers to the chemical or photochemical processes with electron transfer or electron leap. When the oxidants are handled by operators or equipment, generation of static electricity is unavoidable. This index value of thermal stability indicates the safety of these compounds when handled. Energies (eV) of frontier molecular orbital [51, 52] and their gaps ($\Delta E_{LUMO–HOMO}$) of hydrazine derivatives at the same level were shown in Fig. 3. As can be seen, $\Delta E_{LUMO–HOMO}$ values would be different with

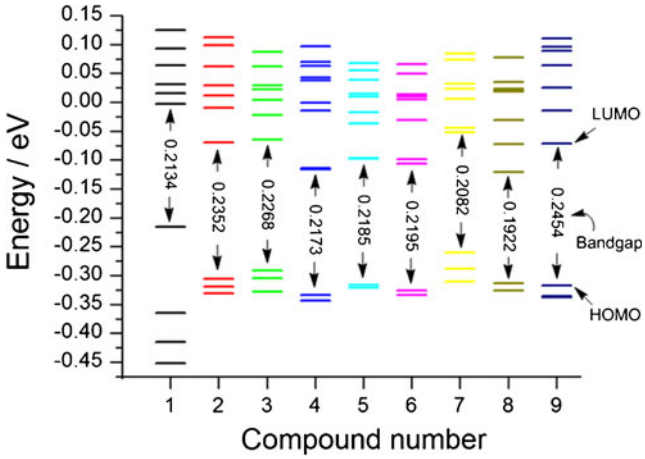

Fig. 3 Energy of highest occupied molecular orbital (E_{HOMO}), energy of lowest unoccupied molecular orbital (E_{LUMO}) and energy gaps ($\Delta E_{LUMO–HOMO}$) of hydrazine derivatives

different substituted groups. The $\Delta E_{LUMO–HOMO}$ of mono-substituted compound (**2** and **3**) was higher than that of di-substituted one (**4**, **5** and **6**). For **4** and **8**, it could be found that two –NO_2 groups at the same position would decrease the value of $\Delta E_{LUMO–HOMO}$ more sharply than at different positions. For **1**, **2** and **9**, the $\Delta E_{LUMO–HOMO}$ increased obviously when reducing the number of –NH_2 groups. Based on these results, we conjectured that the more polarized molecule would own higher $\Delta E_{LUMO–HOMO}$ and thus exhibit greater stability.

The burning rate $\mu(p)$ was relative to the pressure p when oxidants were ignited. This was complex in practice. For example, there was a "platform effect" under the pressure from 1 MPa to 10 MPa in the experimental data of **8**. The method we used could not show all details during the burning process but was exactly in accordance with the change trend. As can be seen in Fig. 4, di-substituted compounds had higher $\mu(p)$ than mono-substituted ones, and their gap obviously increased with pressure. For **4**, **5** and **6**, the –NO_2 group could improve the burning rate more effectively than the HNO_3 group. ADN (**8**), known for its

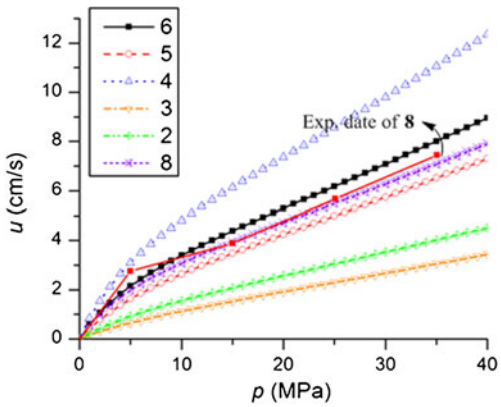

Fig. 4 The calculated burning rate of hydrazine derivatives

astonishingly high burning rate, was one of the most important potential oxidants. Its rate was faster than **5** but fell when compared with **4** and **6**. Considering both the higher oxygen balance and ΔH°_{f} of **4** and **6**, a comprehensive performance of ADN would be inferior to the two designed compounds.

Conclusions

In summary, full geometrical optimizations of oxygen-rich hydrazine derivatives were performed using density functional theory at B3PW91/6−311++G(3df,3pd) level, with no symmetry restrictions. The detailed structure–property studies such as density and volume were conducted based on which energetic performance was studied. By comparing with experimental and calculated data of ammonium nitrate (AN) and ADN, the results proved reliable. Furthermore, stability correlations were established for these compounds by analyzing BDE and energy gaps ($\Delta E_{LUMO-HOMO}$); burning rate was calculated to show their potential application as oxidants in propellants. The simulation results revealed that these hydrazine derivatives have excellent performance and were obviously dominant compared with traditional oxidants. Furthermore, these results provide theoretical support for the molecular design of novel oxidants as well as experimental synthesis.

Acknowledgments We thank the Joint Fund of the National Natural Science Foundation of China and the China Academy of Engineering Physics (NSFC-NSAF No: 11076017) and Scientific Innovation Program of Jiangsu Province (No: CXZZ11_0264) for support of this research.

References

1. Bottaro JC, Penwell PE, Schmitt RJ (1997) 1,1,3,3-Tetraoxo-1,2,3-triazapropene anion, a new oxy anion of nitrogen: the dinitramide anion and its salt. J Am Chem Soc 119:9405–9410
2. Östmark H, Wingborg N, Langlet A (1996) ADN: a new and high performance oxidizer for solid propellants. In: Proceedings of the 16th International Symposium on Ballistics. San Francisco, CA
3. Langlet A, Wingborg N, Östmark H (1997) Challenges in propellants and combustion 100 years after Nobel. Begell House, New York, pp 616–626
4. Chan ML, Reed R, Ciaramitaro DA (2000) Advances in solid propellant formulation. In: Yang V, Brill TB, Ren WZ (eds) Solid propellant chemistry, combustion and motor interior ballistics, progress in astronautics and aeronautics. 185, AIAA, Reston, Chapter1.7
5. Gao H, Shreeve JM (2011) Azole-based energetic salts. Chem Rev 111:7377–7436
6. Gao H, Joo YH, Parrish DA, Vo T, Shreeve JM (2011) 1-Amino-1-hydrazino-2,2-dinitroethene and corresponding salts: synthesis, characterization, and thermolysis studies. Chem Eur J 17:4613–4618
7. Chavez DE, Hiskey MA, Gilardi RD (2004) Novel high-nitrogen materials based on nitroguanyl-substituted tetrazines. Org Lett 6:2889–2891
8. Zarko VE, Anisiforov GI, Kundo NN (2004) Study of the combustion of hydrazinium nitrate based model propellants, energetic material structure and properties. Proceedings of 35th International annual conference of ICT 29.06-2.07, Karlsruhe, FRG, DWS GmbH
9. Manelis GB, Nazin GM, Rubtsov YI, Strunin, VA (2003) Thermal decomposition and combustion of explosive and propellants. Taylor and Francis, London
10. Vasil'ev AA, Valishev AI, Vasil'ev VA, Panfilova LV (2000) Panfilova, Combustion and detonation characteristics of hydrazine and its methyl derivatives. Combust Explo Shock 36:358–373
11. Badgujar DM, Talawar MB, Harlapur SF, Asthana SN, Mahulikar PP (2009) Synthesis, characterization and evaluation of 1,2-bis(2,4,6-trinitrophenyl) hydrazine: a key precursor for the synthesis of high performance energetic materials. J Hazard Mater 172:276–279
12. Schmidt EW (2001) Hydrazine and its derivatives—preparation, properties, application, vol 1–2. Wiley, Chichester
13. Sun HY, Zhang P, Law CK (2012) Ab Initio Kinetics for thermal decomposition of $CH_3N{\bullet}NH_2$, cis-$CH_3NHN{\bullet}H$, trans-$CH_3NHN{\bullet}H$, and $C{\bullet}H_2NNH_2$ radicals. J Phys Chem A 116:8419–8430
14. Mu XG, Wang XJ, Liu XX, Zhang YZ (2012) Thermal decomposition performance of unsymmetrical dimethylhydrazine (UDMH) oxalate. Propell Explos Pyrot 37:316–319
15. Wang SQ, Thynell ST (2012) An experimental study on the hypergolic interaction between monomethylhydrazine and nitric acid. Combust Flame 159:438–447
16. Nusca MJ, Michaels RS (2007) Modeling Hypergolic Ignition in the Army's missile propulsion systems. AIAA 2007–5562, 43rd AIAA/ASME/SAE/ASEE Joint Propulsion Conference and Exhibit, Cincinnati, OH
17. Gengeliczki Z, Borkar SN, Sztaray B (2010) Dissociation of energy-selected 1,1-dimethylhydrazine ions. J Phys Chem A 114:6103–6110
18. Gao JY, Zhang CH, Luo MM, Kim CK, Chu W, Xue Y (2012) Mechanism for the reaction of 2-naphthol with N-methyl-N-phenyl-hydrazine suggested by the density functional theory investigations. J Comp Chem 33:220–230
19. Drake G, Hawkins T, Brand A, Hall L, Mckay M, Vij A, Ismail I (2003) Energetic, low-melting salts of simple heterocycles. Propell Explos Pyrot 28:174–180
20. Zarko VE, Anisiforov GI, Kundo NN, Oparin AV, Keizers H (2004) Study of the combustion of hydrazinium nitrate based model propellants. 35th International Annual Conference of ICT
21. Hooper JB, Borodin O, Schneider S (2011) Insight into hydrazinium nitrates, azides, dicyanamide, and 5-azidotetrazolate ionic materials from simulations and experiments. J Phys Chem A 115:13578–13592
22. Sabat CM, Delalu H, Jeanneau E (2012) Synthesis, characterization, and energetic properties of salts of the 1-cyanomethyl-1,1-dimethylhydrazinium cation. Chem Eur J 7:1085–1095
23. Klapçtke TM, Karaghiosoff K, Mayer KP, Penger A, Welch JM (2006) Synthesis and characterization of 1,4-dimethyl-5-aminotetrazolium 5-nitrotetrazolate. Propell Explos Pyrot 31:188–195
24. Drakem G, Hall L, Hawkins T, Boatz J (2005) Experimental and theoretical study of 1,5-diamino-4-H-1,2,3,4-tetrazolium perchlorate. Propell Explos Pyrot 30:156–163

25. Fan XW, Ju XH, Xiao HM (2008) Density functional theory study of piperidine and diazocine compounds. J Hazard Mater 156:342–347
26. Becke AD (1992) Density functional thermochemistry. II. The effect of the Perdew-Wang generalized gradient correlation correction. J Chem Phys 97:9173–9177
27. Becke AD (1993) Density-functional thermochemistry. III. The role of exact exchange. J Chem Phys 98:5648–5652
28. Perdew JP (1991) In: Ziesche P, Eschrig H (eds) Electronic structure of solids '91. Akademie, Berlin
29. Perdew JP, Chevary JA, Vosko SH, Jackson KA, Pederson MR, Singh DJ, Fiolhais C (1992) Atoms, molecules, solids, and surfaces: applications of the generalized gradient approximation for exchange and correlation. Phys Rev B 46:6671–6687
30. Wong MW, Frisch MJ, Wiberg KB (1991) Solvent effects 1. The mediation of electrostatic effects by solvents. J Am Chem Soc 113:4776–4782
31. Wong MW, Wiberg KB, Frisch MJ (1991) Hartree-Fock second derivatives and electric field properties in a solvent reaction field—theory and application. J Chem Phys 95:8991–8998
32. Klene M, Li X, Knox JE, Hratchian HP, Cross JB, Adamo C, Jaramillo J, Gomperts R, Stratmann RE, Yazyev O, Austin AJ, Camml R, Pomelli C, Ochterski JW, Ayala PY, Morokuma K, Voth GA, Salvador P, Dannenberg JJ, Zakrzewski VG, Dapprich S, Daniels AD, Strain MC, Farkas O, Malick DK, Rabuck AD, Raghavachari K, Foresman JB, Ortiz JV, Cui Q, Baboul AG, Clifford S, Cioslowski J, Stefanov BB, Liu G, Liashenko A, Piskorz P, Komaromi I, Martin RL, Fox DJ, Keith T, Al-Laham MA, Peng CY, Nanayakkara A, Challacombe M, Gill PMW, Johnson B, Chen W, Wong MW, Gonzalez C, Pople JA (2003) Gaussian 03. Gaussian, Inc, Pittsburgh
33. Kamlet MJ, Jacobs ST (1968) Chemistry of detonations. I. A simple method for calculating detonation properties of CHNO explosives. J Chem Phys 48:23–35
34. Lide DR (2002) CRC handbook of chemistry and physics. CRC, Boca Raton
35. Klapötke TM, Schulz A, Harcourt RD (1998) Quantum chemical methods in main-group chemistry, Chap 5. Wiley, Chichester
36. Xu XJ, Xiao HM, Gong XD, Ju XH, Chen ZX (2005) Theoretical studies on the vibrational spectra, thermodynamic properties, detonation properties, and pyrolysis mechanisms for polynitroadamantanes. J Phys Chem A 109:11268–11274
37. Qiu L, Xiao HM, Gong XD, Ju XH, Zhu WH (2006) Theoretical studies on the structures, thermodynamic properties, detonation properties, and pyrolysis mechanisms of Spiro nitramines. J Phys Chem A 110:3797–3807
38. Qiu L, Xiao HM, Ju XH, Gong XD (2005) Theoretical study of the structures and properties of cyclic nitramines: tetranitrotetraazadecalin (TNAD) and its isomers. Int J Quant Chem 105:48–56
39. Xu XJ, Xiao HM, Ma XF, Ju XH (2006) Looking for high-energy density compounds among hexaazaadamantane derivatives with CN, NC, and ONO_2 groups. Int J Quant Chem 106:1561–1568
40. Politzer P, Martinez J, Murray JS, Concha MC, Toro-Labbe A (2009) An electrostatic interaction correction for improved crystal density prediction. Mol Phys 107:2095–2101
41. Lu T, Chen FW (2012) Multiwfn: A multifunctional wavefunction analyzer. J Comp Chem 33:580–592
42. Son S, Brewster (1993) MQ Linear burning rate dynamics of solids subjected to pressure or external radiant heat flux oscillations. J Propul Power 9:222–232
43. Vosen SR (1989) 21th Symposium (International) on Combustion. pp 1817–1825
44. Xiao HM, Fan JF, Go ZM, Dong HS (1998) Theoretical study on pyrolysis and sensitivity of energetic compounds: (3) Nitro derivatives of aminobenzenes. Chem Phys 226:15–24
45. Bickelhaupt FM, Hermann HL, Boche G (2006) α-Stabilization of carbanions: fluorine is more effective than the heavier halogens. Angew Chem Int Edn 45:823–826
46. Redfern PC, Zapol P, Curtiss LA (2000) Assessment of Gaussian-3 and density functional theories for enthalpies of formation of C1-C16 alkanes. J Phys Chem A 104:5850–5854
47. Ball DW (2001) Tetrazane: Hartree-Fock, Gaussian-2 and −3, and complete basis set predictions of some thermochemical properties of N4H6. J Phys Chem A 105:465–470
48. Joseph WO (2000) Thermochemistry in Gaussian. Gaussian Inc, Pittsburgh, PA
49. Curtiss LA, Raghavachari K, Redfern PC, Pople JA (1997) Assessment of Gaussian-2 and density functional theories for the computation of enthalpies of formation. J Chem Phys 106:1063–1079
50. Joseph WO, George AP, Kenneth BW (1995) A comparison of model chemistries. J Am Chem Soc 117:11299–11308
51. Alabugin IV, Manoharan M, Peabody S, Weinhold F (2003) Electronic basis of improper hydrogen bonding: a subtle balance of hyperconjugation and rehybridization. J Am Chem Soc 125:5973–5987
52. Xiao HM, Fan JF, Gong XD (1997) Theoretical study on pyrolysis and sensitivity of energetic compounds. Part I: simple model molecules containing NO_2 Group. Propell Explos Pyrot 22:360–364
53. Manfred AB, Thomas MK (2004) DFT and G2MP2 Calculations of the N–N bond dissociation enthalpies and enthalpies of formation of hydrazine, monomethylhydrazine and symmetrical and unsymmetrical dimethylhydrazine. Z Naturforsch B Chem Sci 59b:148–152
54. McMillen DF, Golden DM (1982) Hydrocarbon bond dissociation energies. Annu Rev Phys Chem 33:493–532